Pergamon

Neurotoxicology and Teratology, Vol. 17, No. 5, pp. 523–530, 1995

0892-0362/95 $9.50 + .00

0892-0362(95)00012-7

Magnetic Resonance Imaging and Spectroscopy in Fetal Ethanol Exposed *Macaca nemestrina*

SUSAN J. ASTLEY,*†[1] EDWARD WEINBERGER,†‡ DENNIS W. W. SHAW,‡ TODD L. RICHARDS,‡ STERLING K. CLARREN†

**Department of Epidemiology, School of Public Health and Community Medicine, †Department of Pediatrics, ‡Department of Radiology, School of Medicine, University of Washington, Seattle, WA 98195*

Received 30 December 1994; Accepted 9 March 1995

ASTLEY, S. J., E. WEINBERGER, D. W. W. SHAW, T. L. RICHARDS AND S. K. CLARREN. *Magnetic resonance imaging and spectroscopy in fetal ethanol exposed Macaca nemestrina.* NEUROTOXICOL TERATOL **17**(5) 523–530, 1995.—Magnetic resonance imaging (MRI) and proton magnetic resonance spectroscopy (^{1}H-MRS) offer noninvasive ways to observe structural and biochemical changes which might serve as valuable diagnostic markers for detecting brain damage from prenatal ethanol teratogenesis. Cranial MR imaging and spectroscopy were performed on 20 nonhuman primates (*Macaca nemestrina*) with known prenatal ethanol exposures and well-documented cognitive and behavioral levels of performance. The choline : creatine ratio detected by ^{1}H-MRS in the brain increased significantly with increasing duration of in utero ethanol exposure. These signal alterations occurred in the absence of gross structural brain anomalies (detectable by MRI) and were significantly correlated with alcohol-related cognitive and behavioral dysfunction. These observations are consistent with reports of elevated choline : creatine ratios associated with various neurologic insults and disease states. The association observed between brain choline : creatine ratios and in utero ethanol exposure suggest a role for ^{1}H-MRS in elucidating mechanisms of ethanol teratogenicity.

Fetal alcohol syndrome (FAS) Magnetic Resonance Imaging (MRI) Magnetic Resonance Spectroscopy (MRS) Cholinergic Acetylcholine

A PREVIOUS report has demonstrated that ethanol teratogenicity in nonhuman primates (*Macaca nemestrina*) can result from just once per week binge drinking in only the first 6 to 8 weeks of gestation (5). This exposure can produce cognitive and behavioral abnormalities with or without associated abnormalities in growth or facial form. Magnetic resonance imaging (MRI) and proton spectroscopy (^{1}H-MRS) offer noninvasive ways to observe structural and biochemical changes that might serve as valuable diagnostic markers for detecting brain damage from prenatal ethanol teratogenesis. Cranial MR imaging and spectroscopy were performed on a group of nonhuman primates with known prenatal ethanol exposures and well-documented cognitive and behavioral levels of performance (5,6) to test the usefulness of this technology in this disorder.

METHOD

Study Population, Maternal Dosing, and Infant Developmental Assessment

Cranial MRI and ^{1}H-MRS were performed on the offspring of 20 nonhuman primates (*Macaca nemestrina*) who were prenatally exposed to ethanol or sucrose (control) solution. The mothers of the offspring were time-mated over a period of 1.9 years and randomly assigned to one of four exposure groups. The dams in Group 1 received 1.8 g/kg ethanol once a week for the entire 24 weeks of pregnancy. Group 2 received a sucrose solution that was isocaloric and isovolemic to the ethanol solution once a week for the entire 24 weeks of pregnancy. Group three received the ethanol solution once a week for Weeks 1 through 3 and the sucrose solution

[1] Requests for reprints should be addressed to Susan J. Astley, Ph.D., Division of Congenital Defects, Children's Hospital and Medical Center, CH-47, 4800 Sand Point Way N.E., Seattle, WA 98105.

once a week for Weeks 4 through 24. Group 4 received the ethanol solution once a week for Weeks 1 through 6 and the sucrose solution once a week for Weeks 7 through 24. The ethanol and sucrose solutions were administered orally via a soft nasogastric tube. Dosing was always initiated on the same day of the week, resulting in seven different weekly dosing schedules relative to the day of conception [i.e., gestational days (GDs) 1, 8, 15...; GDs 2, 9, 16...; through GDs 7, 14, 21...]. The distribution of the seven dosing schedules was comparable across the four exposure groups.

MRI and ^{1}H-MRS were conducted in the fall of 1993 when the offspring were between 2.4 and 4.1 years of age (the human equivalent of early to late adolescence). These 20 offspring are the survivors of a larger group of offspring (n = 27) assessed in the original ethanol teratogenicity study (5). They include six offspring in the control group, five in the 3-week ethanol group, five in the 6-week ethanol group, and four in the 24-week ethanol group. A summary of the developmental outcomes, through 6 months of age, for each offspring are presented by animal study number in Fig. 1 in Clarren et al. (5). The offspring included in this MRI/S study include animal numbers 34 through 60, excluding animal numbers 39, 42, 47, 53, 54, 57, and 59. Care and handling of all animals was in accordance with institutional guidelines.

Maternal peak plasma ethanol concentrations were monitored on all dams within 1 week postpartum. The mean peak plasma ethanol concentration among the 14 ethanol exposed animals was 227 ± 33 mg/dl, a level that could be achieved by a 55 kg person consuming approximately 6 to 8 beers or its equivalent. Peak plasma ethanol concentrations were monitored in the postpartum period to minimize handling during pregnancy. Pre- and postpartum plasma ethanol concentrations were confirmed to be comparable (6). Maternal dosing, pregnancy management, and pregnancy outcomes are presented in detail in Clarren & Astley (6).

Infant motor, cognitive, behavioral, and physical development was documented from birth through 24 months of age with a comprehensive battery of assessments which were developed and have been administered at the Infant Primate Research Laboratory for over 20 years (5). Briefly, 5- and 10-min Apgar scores were obtained and a complete physical examination was conducted at birth. Early motor and behavioral reflex responses were monitored from birth through 3 weeks of age using an adaptation of the Brazelton Neonatal Behavioral Assessment Scale (2). Attention, discrimination, and memory abilities were monitored between 2 and 4 weeks of age with an adaptation of the Fagan Test of Human Infant Intelligence (14). Motor and behavioral development during social interaction with age-matched peers in a playroom was recorded twice weekly from three weeks to nine months of age. Object permanence conceptualization, the ability to perceive objects as permanent entities when removed from site, was monitored twice weekly from 3 weeks to 4 months of age using the Object Permanence Test Series. Learning and memory skills were tested daily from 4 to 14 months of age using the Wisconsin General Testing Apparatus (WGTA) (18). Measures of activity and distraction were recorded during all WGTA test sessions. Free-play activity level in an observation playroom was recorded and coded on videotape at 1, 6, and 12 months of age. Infant growth and craniofacial development was documented through anthropometric examination and collection of standardized cephalometric X-rays and photographs at 1, 6, 12, and 24 months of age. Detailed descriptions of infant rearing, assessment, and developmental outcomes through the first 6 months of life can be found in Clarren et al. (5,7).

In this MRI/S study, an unweighted composite score reflecting each animal's developmental impairment through 6 months of age was derived by dividing the number of assessments an animal failed by the number of assessments used to summarize each animals' development in Fig. 1 presented in Clarren et al. (5). Failure for each assessment was defined as

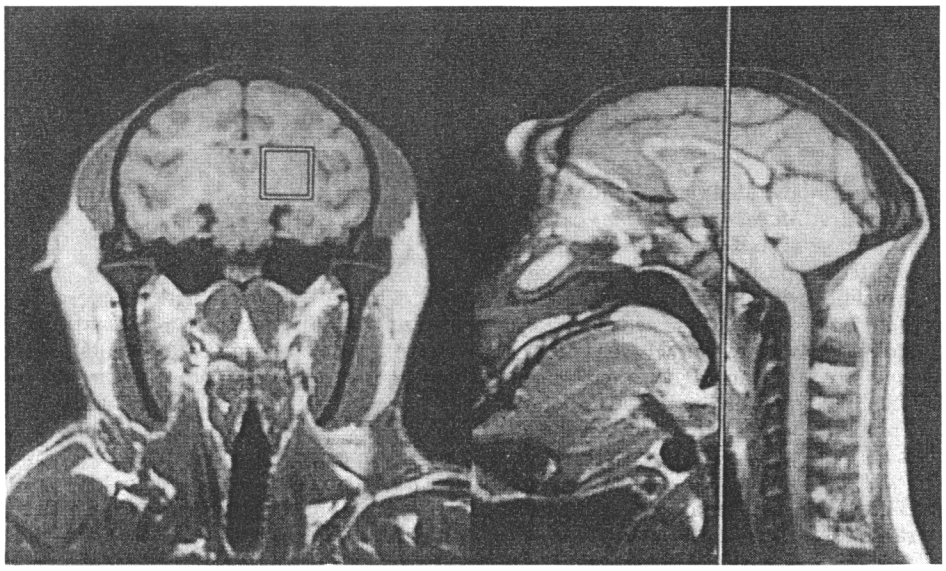

FIG. 1. Coronal and sagittal T1-weighted magnetic resonance images (400–550/12, repetition/echo times in ms), defining the region of interest for magnetic resonance spectroscopy. The center of the 3.4 cc volume of interest was selected on a coronal image selected from a sagittal localizer to include thalamus, parts of the internal capsule and basal ganglia, and adjacent white matter.

(a) performance > 2 SDs below the mean performance of the control animals or (b) presence of a neurologic disorder/congenital anomaly.

MRI and ^{1}H-MRS

MRI and ^{1}H-MRS were carried out on a General Electric Signa whole body MR Scanner operating at 1.5 Telsa, using version 4.6 software and hardware. The animals were sedated with an intramuscular injection of ketamine/xylazine (10 mg/kg), placed in prone position, and aligned comparably (Frankfort Horizontal plane at 90°; to the horizontal axis of the scanner) in a knee coil with the aid of a custom designed stereotaxic head holder. A knee coil was used to accommodate the small size of the animals' heads. Although blood gas or oximetry data was not collected, respiration was visually monitored and postioning in the Frankfort Horizontal alignment facilited maintanence of a free airway. MRI and ^{1}H-MRS were obtained sequentially utilizing the same hardware. The entire procedure (alignment, imaging, and spectroscopy) required approximately 60 min of sedation time.

The MRI study was performed first and included T1-weighted sequences in the sagittal and coronal planes, and both T1 and T2-weighted images in the axial plane. Sequence parameters for T1-weighted images were repetition time (TR) 400–550 ms and echo time (TE) 12 ms. Parameters for T2-weighted images were TR 2500 ms and TE 23 and 80 ms. A 16-cm field of view was utilized with slice thickness of 3 or 4 mm.

MR coronal images were used to define a 3.4 cc brain region of interest for spectroscopy (Fig. 1). Volume-localized spectra were achieved using the point resolved spectroscopy (PRESS) pulse sequence (27). This pulse sequence uses 90°–180°–180° radio frequency pulses and has three water suppression radio frequency pulses with gradient spoilers. Magnetic field homogeneity was adjusted with the *X*, *Y*, and *Z* gradients using the localized voxel immediately before spectral data acquisition. The acquisition parameters were: TR 2000 ms; TE 136 ms; voxel size 3.4 cc; sweep width of 1000 Hz; spectral frequency 63.8 MHz; number of acquisition points 1024; number of averages 100.

The above parameters result in acquisition of spectra with three principle resonances: choline-containing compounds (Cho), creatine-containing compounds (Cr), and N-acetyl aspartate (NAA) (Fig. 2A). The *N*-methyl groups of choline containing compounds resonate at 3.2 ppm in the MR spectra, Cr resonates at 3.0 ppm and the *N*-methyl group of NAA resonates at 2.0 ppm. Cho is a precursor for the neurotransmitter acetylcholine and for phosphatidylcholine and sphingomyelin, two common phospholipids in neuronal and glial membranes (25). NAA is relatively abundant in neural tissue and is believed to be involved in regulation of neuronal protein synthesis, myelin production, and the metabolism of several neurotransmitters such as aspartate and N-acetyl-aspartyl-glutamate (1). Both creatine and creatine phosphate contribute to the single creatine peak. Creatine serves as a reserve for high-energy phosphates in the cytosol of muscle and neurons and buffers cellular ATP/ADP reservoirs. The integrated areas of the ab-

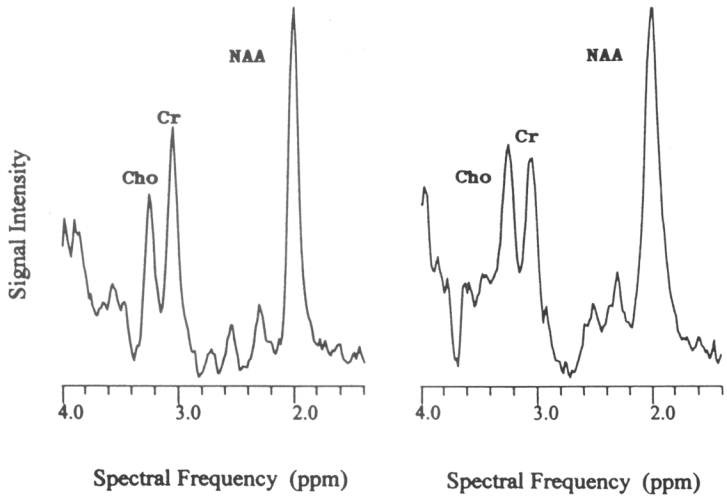

FIG. 2. A. Magnetic resonance spectrum, 2000/136 (repetition/echo time in msec), with the water signal suppressed, of a 3.4 cc brain tissue volume from a control animal (#37) and a 24-week ethanol exposed animal (#56). The Cho/Cr ratio (0.66) for the control animal is reflective of the group mean. The Cho/Cr ratio for the ethanol-exposed animal (0.95) was the highest observed ratio. choline (Cho), creatine (Cr), N-acetyl-aspartate (NAA). B. Baseline corrected spectra for the Cho, Cr, and NAA regions of the proton magnetic resonance spectra for the two animals presented in A. The solid line is the actual spectral data and the shaded line is the fit. The baseline was determined at constant ppm regions near the resonances for all the spectra and then fit to a linear equation. The baseline was subtracted from the spectrum before fitting was performed. Fitting was performed using a superposition of two resonances in the Gaussian equation for the Cho/Cr region and a single resonance Gaussian equation for the NAA region of the spectrum. The resonance areas were determined from the height and width resulting from the fit. choline (Cho), creatine (Cr), N-acetyl-aspartate (NAA).

sorption-mode resonances (peak areas) for Cho, Cr, and NAA were computed using Lorenzian/Gaussian peak-fitting software after automated baseline subtraction (Fig. 2B). Best fit was achieved using a 100% Gaussian distribution. Proton spectra were quantified by dividing the peak area of the metabolite of interest by the peak area of another metabolite in the spectrum providing relative rather than absolute measures of metabolite concentration. Because past studies have demonstrated that the creatine peak is relatively stable with various diseases, it is often used as a control value, with some limitations, to compare with changes seen in NAA and Cho (3).

Analysis

The MR images were reviewed for the presence of gross morphologic anomalies by two radiologists (EW, DWS) and a dysmorphologist (SKC), masked to the exposure history of the animals. Computer-aided volumetric analyses were not conducted. One-way analysis of variance (ANOVA) and Student-Newman-Keuls test for multiple comparisons were used to determine if significant differences in mean ^{1}H-MRS metabolite ratios and mean infant developmental impairment composite scores could be detected between the four ethanol exposure cohorts. Regression analysis was used to evaluate the relationship between ^{1}H-MRS metabolite ratios, gestational day of ethanol exposure, and composite scores of infant developmental impairment through 6 months of age.

RESULTS

Review of the MR images revealed no gross morphologic abnormalities of CNS structures among any of the animals. No gross differences in morphology or size of cerebral hemispheres, corpus callosum, brainstem, or cerebellum were visually detectable between the animals.

MRS revealed a statistically significant increase in the Cho : Cr ratio with increasing duration of in utero ethanol exposure (one-way ANOVA weighted linear trend: $F(3, 16) = 10.2, p = 0.006$ (Table 1, Fig. 3a). The 24-week ethanol cohort had a significantly higher mean Cho : Cr metabolite ratio relative to the control and 3-week ethanol cohorts (Student-Newman-Keuls multiple comparison test: $p < 0.05$). These results closely parallel the significant linear association observed between the infant developmental impairment scores and duration of ethanol exposure in which both the 6- and 24-week ethanol exposed cohorts differed significantly from the control group (one-way ANOVA weighted linear trend: $F(3, 16) = 6.8, p = 0.02$; Student-Newman-Keuls multiple comparison test: $p < 0.05$) (Fig. 3b). Although the increase in the Cho : Cr ratio could be due to an increase in Cho and/or a decrease in Cr, analyses of the ratios NAA : Cr and NAA : Cho strongly suggest that it is the Cho component that is changing with increasing duration of ethanol exposure, not the Cr.

No statistically significant associations were observed between the NAA : Cr and Cho : NAA metabolite ratios and duration of in utero ethanol exposure. Although the power to detect statistically significant associations was limited by the small number of animals in each group, the negative statistical results were supported by the lack of any pattern of association observed in the scatter plots (not illustrated).

Metabolite ratios did not vary with gender, age at the time of the MR evaluation, total dose of ketamine : xylazine/kg body weight, or gestational age at first dose of ethanol.

A scatter plot of the Cho : Cr ratios and the developmental impairment composite scores revealed a significant curvilinear relationship with 45% of the variance in the impairment score being explained by the Cho : Cr ratio ($r^2 = 0.45$; $F = 6.9$, $p = 0.006$). The curvilinear nature of the plot was dominated by the outcome of a single animal (animal #49) in the 6-week exposure cohort (identified by an asterisk in Fig. 4). This animal was the most developmentally delayed animal in the study and was the only animal with a Cho : Cr ratio greater than 2 SDs below the control mean. If the outlier is excluded from the analysis, the developmental impairment score increases linearly with increasing Cho : Cr ratio with 34% of the variance in the developmental outcome score being explained by the Cho : Cr ratio ($r^2 = 0.34$, $F = 8.6$, $p = 0.009$).

DISCUSSION

Results demonstrated brain Cho : Cr ratios detected by ^{1}H-MRS increased with increasing duration of in utero ethanol

TABLE 1

SUMMARY OF DESCRIPTIVE CHARACTERISTICS AND OUTCOMES ACROSS THE FOUR ETHANOL EXPOSURE COHORTS

	Duration of Once-Per-Week Maternal Ethanol Exposure During Pregnancy			
Characteristics	0 weeks	3 weeks	6 weeks	24 weeks
	(n = 6)	(n = 5)	(n = 5)	(n = 4)
Metabolite ratios, mean (SE)				
Cho : Cr*	0.66 (0.03)	0.67 (0.05)	0.72 (0.06)	0.85 (0.04)
NAA : Cr	2.01 (0.24)	1.63 (0.06)	1.95 (0.19)	2.07 (0.39)
Cho : NAA	0.34 (0.02)	0.41 (0.04)	0.37 (0.02)	0.44 (0.05)
Infant Developmental Outcome Scores†, mean (SE)	0.03 (0.02)	0.15 (0.05)	0.31 (0.09)	0.27 (0.04)
Female (n)	6	2	3	3
Age in years at time of MRI/^{1}H-MRS, mean (SE)	3.6 (0.2)	3.2 (0.2)	3.8 (0.1)	3.1 (0.3)
Age in days at first treatment dose, mean (SE)	— —	6.6 (1.1)	8.8 (1.2)	9.5 (1.3)
Ketamine : xylazine dose (mg/kg) mean (SE)	0.25 (0.05)	0.22 (0.03)	0.19 (0.01)	0.20 (0.03)

*One-way ANOVA weighted linear trend: $F(3, 16) = 10.2$, $p = 0.006$. Student-Newman-Keuls multiple comparison test: 24-week cohort differs from the control and 3-week cohort, $p < 0.05$. † One-way ANOVA weighted linear trend: $F(3, 16) = 5.8$, $p = 0.02$. Student-Newman-Keuls multiple comparison test: 6- and 24-week cohorts differ from the control group, $p < 0.05$. SE = Standard Error.

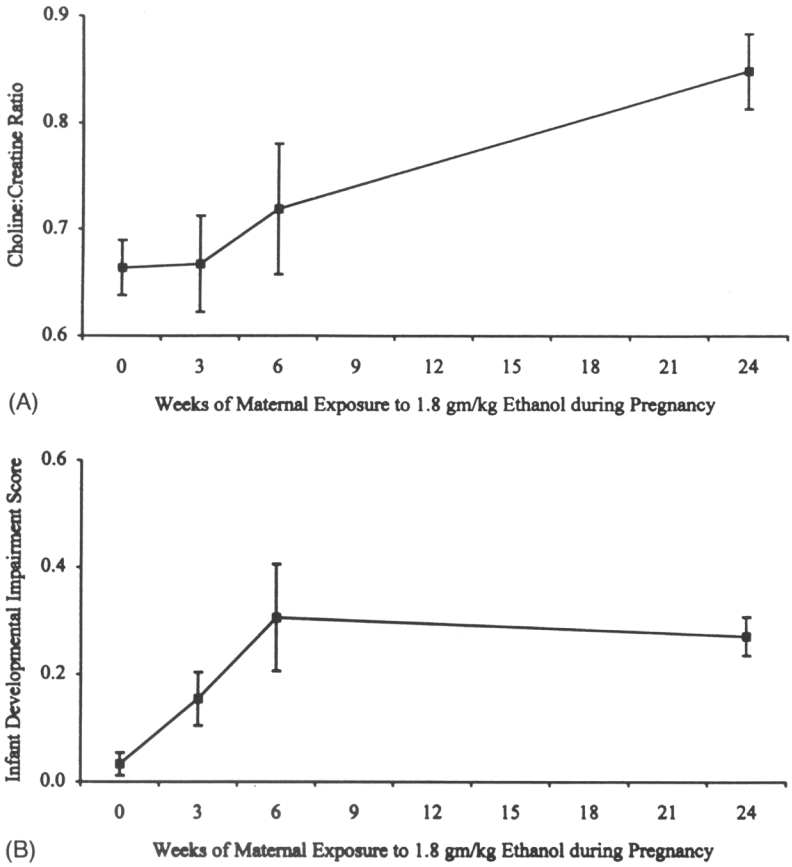

FIG. 3. A. Mean (±SE) brain choline : creatine ratios for the control, 3-week, 6-week, and 24-week ethanol exposure cohorts. The mean Cho : Cr metabolite ratio increased linearly with increasing duration of ethanol exposure (Oneway ANOVA weighted linear trend: $F(3, 16) = 10.2$, $p = 0.006$). B. Mean (±SE) infant developmental impairment score for the control, 3-week, 6-week, and 24-week ethanol exposure cohorts. The mean infant developmental impairment score increased linearly with increasing duration of ethanol exposure (one-way ANOVA weighted linear trend: $F(3, 16) = 6.8$, $p = 0.02$).

exposure, $F(3, 16) = 10.2$; $p = 0.006$, in this nonhuman primate model of fetal alcohol syndrome (FAS). These alterations occur in the absence of gross morphological abnormalities among live born animals (detectable by MR imaging). The Cho : Cr ratios were also observed to increase with increased cognitive and behavioral dysfunction in these animals ($r^2 = 0.45$; $F = 6.9$, $p = 0.006$). The observed increase in the Cho : Cr ratio is consistent with reports of elevated Cho : Cr ratios associated with various neurological insults and disease states (e.g., brain ischemia, brain tumors, multiple sclerosis, and Alzheimer's disease) (4,21,26,31,23). The absence of gross morphological abnormalities is consistent with observations in our previous study of ethanol teratogenicity in nonhuman primates (8). Morphological abnormalities such as agenesis of the corpus callosum have been reported in a few FAS case-series (9,19,22) but the prevalence appears to be quite low.

The Role of Choline and Detection by ^{1}H-MRS

Choline is a precursor for two important molecules, phosphatidylcholine (PtdCho) and acetylcholine (AcCho). Cho is present in membranes of all cells, where it constitutes the polar subunit of PtdCho, sphingomyelin, and plasmalogens. Within cholinergic neurons, Cho is also the precursor for the synthesis of AcCho (16). The rate of AcCho synthesis is regulated by the concentration of substrate Cho in cholinergic neurons. Choline acetyltransferase (CAT) catalyzes the synthesis of AcCho in the reaction: Cho + acetyl coenzyme A → AcCho + coenzyme A. AcCho is a neurotransmitter that is critical for many aspects of memory, cognition, and mood (13).

There remains uncertainty in the field of MR spectroscopy as to which of the choline containing compounds contribute to the 3.2 ppm peak. The total concentration of the major water soluble choline containing compounds including choline, glycerophosphocholine, phosphorylcholine, CDP-choline, AcCho, and choline-plasmalogen total to less than 1.6 mM (25). Conversely, lipid-soluble sphingomyelin and PtdCho occur in concentrations that are over 20 mM, but the proton spectrum of "normal" brain has little (if any) lipid signal because the phospholipids in cell membranes have limited mobility (37,15). It is believed that the choline peak seen in ^{1}H-MRS reflects all choline stores but is most likely dominated by sig-

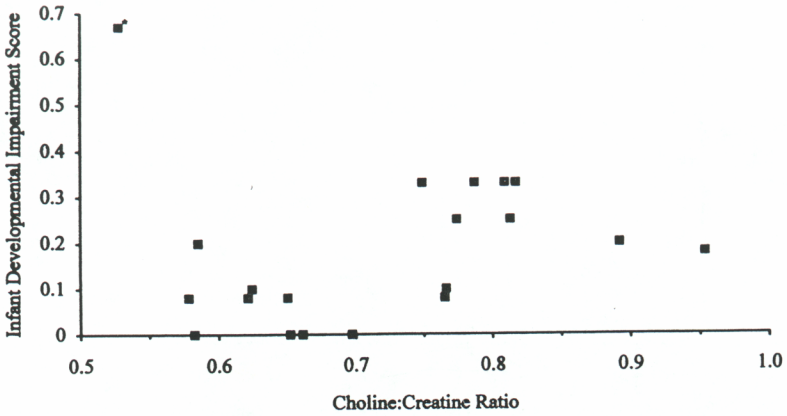

FIG. 4. Scatterplot of the the brain Cho/Cr ratios detected by ^{1}H-MRS and the developmental impairment composite scores. There is a significant curvilinear relationship with 45% of the variance in the impairment score being explained by the Cho : Cr ratio ($r^2 = 0.45$; $F = 6.9$, $p = 0.006$). The curvilinear nature of the plot was dominated by the outcome of a single animal in the 6-week exposure cohort (identified by an asterisk), which may be suggestive of a threshold effect. If the outlier is excluded from the analysis, the developmental impairment score increases linearly with increasing Cho : Cr ratio with 34% of the variance in the developmental outcome score being explained by the Cho : Cr ratio ($r^2 = 0.34$, $F = 8.6$, $p = 0.009$). choline (Cho) creatine (Cr).

nal from lipids being mobilized for membrane synthesis (e.g., brain tumor growth) or breakdown (e.g., demyelination observed in multiple sclerosis).

Cholinergic-based research in Alzheimer's Disease (AD) provides supportive evidence that the choline peak seen in ^{1}H-MRS may indeed be reflective of membrane destabilization. In AD, cortical AcCho and CAT levels are significantly reduced relative to age-matched controls (11,38). As noted, the rate of AcCho synthesis is regulated by the concentration of substrate Ch in cholinergic neurons. The decline of cortical AcCho in AD is attributed to the selective loss of cholinergic neurons, particularly from the cholinergic pathway projecting from deep nuclei located in the septum near the diagonal band of Broca to the hippocampus and from the nearby basal nucleus of Meynert to the cerebral cortex (10) (Fig. 5). Wurtman et al. (39) hypothesized that Cho deprived cholinergic neurons catabolize their own membranes ("autocannabalism") to free-up Cho for AcCho synthesis. Wurtman et al. suggest that this dual use of Cho for membrane and neurotransmitter synthesis could make AcCho producing cells particularly vulnerable to alterations in Cho levels. In a recent ^{1}H-MRS study, Meyeroff et al. (23) observed significantly higher Cho/Cr signals in patients with AD relative to elderly controls. Cho/Cr was 37% higher ($p = 0.0002$) in the mesial gray matter of the centrum semiovale and 23% higher ($p = 0.05$) in adjacent lateral voxels located in a predominantly white matter region of the posterior cortex. The authors note the consistency of their observations with reports in the AD literature document-

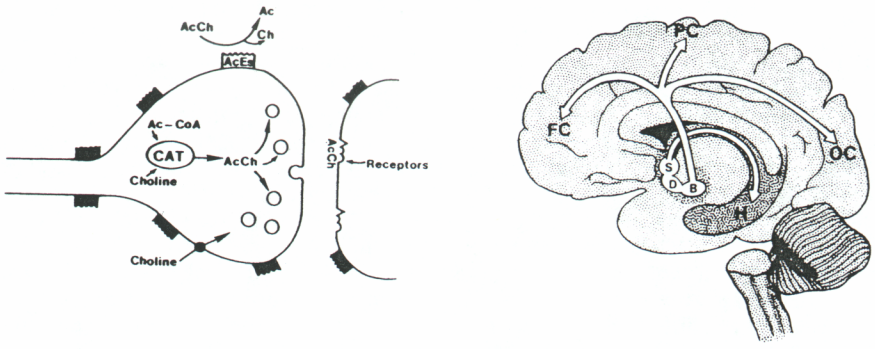

FIG. 5. Cholinergic pathways innervating cortex. The cholinergic neuronal cell bodies of the basal forebrain located in the nucleus basilis of Meynert (B), the diagonal band of Broca (D), and the medial septal nucleus (S) send axons that innervate the entire cortex including the frontal (FC), parietal (PC), and occipital (OC) cortex, as well as the hippocampal formation (H). (Reprinted with permission by Coyle et al., 1983).

ing membrane degradation effects due to increased phospholipid turnover (28,29) and defective membrane lipid compositions associated with membrane bilayer destabilization (17). As Meyerhoff et al. state, these observations are unified by Wurtman's "autocannabalism" theory on the pathogenesis of AD.

Depletion of Cholinergic Nuclei in a Mouse Model of FAS

Although limited work has been focused on the cholinergic system in FAS research, a recent study in mice has confirmed that in utero ethanol exposure can cause severe depletion of cholinergic nuclei (32). In that study, C57B1/6J mice were given two doses of ethanol (2.9 g/kg maternal body weight per dose, 500–600 mg/dl maternal peak blood alcohol concentration) on GD 7. In the mildly affected brains of GD 18 fetuses, fewer cells were immunoreactive for CAT in the medial septal nucleus and the vertical and horizontal nucleus of the diagonal band of Broca. In the severely affected brains, cells immunoreactive to CAT were totally absent. The severely affected mice had craniofacial anomalies consistent with those observed in humans with FAS. Schambra reports that without the projections of cholinergic neurons of the medial septal nucleus and the vertical nucleus of the diagonal band of Broca to the hippocampus, memory deficits as well as difficulty in inhibiting unwanted behaviors can be expected, as is reported to occur in FAS humans.

Although Schambra (32) and Sulik (34,35) have identified GD 7 in the mouse (Stage 9 of embryonic development, gastrulation) as a critical stage when acute exposure to ethanol can result in medial forebrain anomalies and FAS-like facial dysmorphia, the outcomes observed in this non human primate study cannot be isolated to a single stage of development because ethanol was administered weekly. There is one event, however, that was observed in this study that not only suggests that timing of exposure may be an important factor related to outcome but also provides a link between the outcomes observed in Schambra's study and the outcomes observed in this study. Schambra (32) and Sulik (35,35) report a continuum of ethanol induced teratogenic damage with holoprosencephaly representing the severe end of the spectrum. Sulik (36) goes on to speculate that severe cases of FAS represent the mild end of the holoprosencephaly spectrum. In this group of non human primates, one ethanol exposed animal was born with holoprosencephaly (33), an event that has never before been reported in the non human primate literature. Only one other animal (animal #56) in this MRI/S study had a weekly dosing pattern that was identical in timing (GDs 12, 21, 26 . . .), level, and duration to the holoprosencephalic animal. That animal had the highest Cho : Cr ratio of the group, a ratio that was 4.8 SDs higher than the control mean. Stage 9 of embryonic development in man (30) and macaque is estimated to occur at 20 ± 1 days postovulation.

Area Localized for ^{1}H-MRS

The majority of cortical cholinergic innervation is derived from nerve cells in the basal forebrain (20). The primary source of cortical cholinergic innervation in the rat originate from neurons in the ventral and medial aspects of the *globus pallidus*, extend into the hypothalamus and range rostrally to include the diagonal band of Broca and the medial septal nucleus (12). These areas correspond to the areas of cholinergic nuclei depletion observed in the FAS mouse model following in utero ethanol exposure (32). Comparative neuroanatomic studies indicate that the major part of this cholinergic system in primates is located in the nucleus basilis of Meynert (22) (Fig. 5), an area that was incorporated in the 3.4 cc voxel localized for ^{1}H-MRS in this primate study.

Based on the mechanism of cholinergic membrane vulnerability postulated by Wurtman et al. (39) one could speculate that the increased Cho : Cr ^{1}H-MRS signal ratios observed in this study may be associated with membrane breakdown. If AcCho is deficient, as might be expected based on the type of cognitive/behavioral impairment which is characteristic of patients with FAS (and is confirmed to be present in these nonhuman primates), breakdown of cholinergic neuron membranes could serve as a compensatory measure to free up Cho for AcCho synthesis. As demonstrated by Tunggal et al. (37), choline from catabolism of membrane phospholipids might considerably contribute to the AcCho neurotransmitter pool of the CNS. If cholinergic membranes were breaking down, one would expect to observe elevated Cho : Cr ^{1}H-MRS signals.

Interestingly, the only animal that deviated from the pattern of increased Cho : Cr signal with increased cognitive impairment was animal #49, the animal with the most profound cognitive and behavioral impairment and the only live born animal with minor facial dysmorphia. One could speculate that this animal may have sustained a level of damage that was beyond that of the other animals, perhaps severe enough to result in depletion of cholinergic nuclei. In such case, compensatory measures such as membrane breakdown would be less successful at achieving adequate AcCho levels and would result in a lower Cho : Cr MRS signal, as was observed. Ongoing neuroanatomical and neurochemical studies may shed light on the apparent uniqueness of this individual animal.

In conclusion, the association observed between brain Cho : Cr ratios and in utero ethanol exposure suggest a role for ^{1}H-MRS in elucidating mechanisms of ethanol teratogenicity. There may further be diagnostic benefits derived from the metabolic information available from ^{1}H-MRS in evaluation of FAS. These findings add further weight to the developing body of knowledge that purport that behavioral abnormalities can be attributable to prenatal exposure to ethanol in utero without evidence of microcephaly or structural aberration at the resolution level of CT or MR imaging. To our knowledge, this is the first reported association between in utero ethanol exposure and cranial Cho : Cr ratios detected by ^{1}H-MRS. Although further study is required to confirm this association, the dose-response nature of the association and documented cholinergic vulnerability in other animal models of FAS lend credence to this observed association.

ACKNOWLEDGEMENTS

We thank Douglas M. Bowden and the staff at the University of Washington Regional Primate Research Center (RPRC), the Infant Primate Research Laboratory, and the Child Development and Mental Retardation Center for their support of this study and the RPRC Bioengineering Division their help in the design and construction of the MRI stereotaxic head-holder. We also thank the staff of the University of Washington MRI Diagnostic Laboratory for the use of their facilities and expertise in conducting this study.

This research was supported in part by grants from General Electric (No. R32672.17) and the USPHS (AA05616).

REFERENCES

1. Birken, D. L.; Oldendorf, W. H. N-acetyl-L-aspartic acid: A literature review of a compound prominent in ^{1}H-NMR spectroscopic studies of brain. Neurosci. Behav. Rev. 13:23–31; 1989.
2. Brazelton, T. B. Neonatal behavioral assessment scale, 2nd ed. Philadelphia, PA: J.B. Lippincott; 1983.
3. Brenner, R. E.; Munro, P. M. G.; Barker, G. J.; Hawkins, C. P.; Landon, D. N.; McDonald, W. I. The proton NMR spectrum in acute EAE: The significance of the change in the Cho : Cr ratio. Magn. Res. Med. 29:737–745; 1993.
4. Bruhn, H.; Frahm, J.; Gyngell, M. L.; Merboldt, K. D.; Hanicke, W.; Sauter, R. Cerebral metabolism in man after acute stroke: New observations using localized proton NMR spectroscopy. Magn. Res. Med. 9:126–131; 1989.
5. Clarren, S. K.; Astley, S. J.; Gunderson, V. M.; Spellman, D. Cognitive and behavioral deficits in nonhuman primates associated with very early embryonic binge exposures to ethanol. J. Pediat. 121:789–796; 1992.
6. Clarren, S. K.; Astley, S. J. Pregnancy outcomes after weekly oral administration of ethanol during gestation in the pig-tailed macaque: Comparing early gestational exposure to full gestational exposure. Teratol. 42:1–9; 1992.
7. Clarren, S. K.; Astley, S. J.; Bowden, D. M. Physical anomalies and developmental delays in non human primate infants exposed to weekly doses of ethanol during gestation. Teratology 37:561–569; 1988.
8. Clarren, S. K.; Astley, S. J.; Bowden, D. M.; Lai, H.; Milam, A. H.; Rudeen, P. K.; Shoemaker, W. J. Neuroanatomic and neurochemical abnormalities in nonhuman primate infants exposed to weekly doses of ethanol during gestation. Alc. Clin. Exp. Res. 14:674–683; 1990.
9. Clarren, S. K. Neuropathology in fetal alcohol syndrome. In: West, J. R., ed. Alcohol and brain development. New York: Oxford University Press; 1986:158–166.
10. Coyle, J. T.; Price, D. L.; DeLong, M. R. Alzheimer's disease: A disorder of cortical cholinergic innervation. Science 219:1184–1190; 1983.
11. Davies, P.; Maloney, A. J. F. Selective loss of central cholinergic neurons in Alzheimer's disease. Lancet 2:1402; 1976.
12. Divac, I. Magnocellular nuclei of the vasal forebrain project to neocortex, brainstem, and olfactory bulb. Review of some functional correlates. Brain Res. 93:385–398; 1975.
13. Drachman, D. A. Memory and cognitive functions in man: Does the cholinergic system have a specific role? Neurology 27:783–790; 1977.
14. Fagan, J. F.; Singer, L. T. Infant recognition memory as a measure of intelligence. In: Lipsitt, L. P., ed.: Advances in infancy research, Vol. 2. Norwood, NJ: Ablex Press; 1983:31.
15. Frahm, J..; Bruhn, H.; Gyngell, M. L.; Merbosdt, K. D.; Hanicke, W.; Sauter, R. Localized high-resolution proton NMR spectroscopy using stimulated echoes: Initial applications to human brain in vivo. Magn. Res. Med. 9:79–93; 1989.
16. Freeman, J. J.; Jenden, D. J. The source of choline for acetylcholine synthesis in brain. Life Sci. 19:949–962; 1976.
17. Ginsberg, L.; Atack, J. R.; Rapoport, S. I.; Gershfeld, N. L. Regional specificity of membrane instability in Alzheimer's disease brain. Brain Res. 615:355–357; 1993.
18. Harlow, H. F. The development of learning in the rhesus monkey. American Scientist 47:459–479; 1959.
19. Jeret, J. S.; Serur, D.; Wisniewski, K. E.; Lubin, R. A. Clinicopathological findings associated with agenesis of the corpus callusum. Brain Dev. 9:255–264; 1987.
20. Johnston, M. V.; McKinney, M.; Coyle, J. T. Evidence for a cholinergic projection to neocortex from neurons in basal forebrain. Proc. Natl. Acad. Sci. USA 77:5392–5396; 1976.
21. Luyten, R. P.; Marien, A. J.; Heindel, W.; Van Gerwen, P. H.; Herholz, K.; den Hollander, J. A.; Friedman, G.; Heiss, W. D. Metabolic imaging of patients with intracranial tumors: H-1 MR spectroscopic imaging and PET. Radiology 176:791–799; 1990.
22. Mattson, S. N.; Riley, E. P.; Jernigan, T. L.; Ehlers, C. L.; Delis, D. C.; Jones, K. L.; Stern, C.; Johnson, K. A.; Hesselink, J. R.; Bellugi, U. Fetal alcohol syndrome: A case report of neuropsychological, MRI, and EEG assessment of two children. Alc. Clin. Exp. Res. 16:1001–1003; 1992.
23. Meyeroff, D. J.; MacKay, S.; Constans, J. M.; Norman, D.; Van Dyke, C.; Fein, G.; Weiner, M. W. Axonal injury and membrane alterations in Alzheimers Disease suggested by in vivo proton magnetic resonance spectroscopic imaging. Ann. Neurol. 36:40–47; 1994.
24. Meynert, T.; vom Gehirn der Saugetiere. In: Handbuch der Lehre von den Geweben des Menschen und Thiere. S. Stricker, Ed. (Engelmann, Leipzig, 1872), Vol. 2: p. 694.
25. Miller, B. L. A review of chemical issues in ^{1}H-NMR spectroscopy: N-acetyl-L-aspartate, creatine and choline. NMR in Biomedicine 4:47–52; 1991.
26. Miller, D. H.; Austin, S. J.; Connelly, A.; Youl, B. D.; Gadian, D. G.; McDonald, W. I. Proton magnetic resonance spectroscopy of an acute and chronic lesion in multiple sclerosis. Lancet 337: 58–59; 1991.
27. Moonen, C. T. W.; von Kienlin, M.; van Zijl, P. C. M.; Cohen, J.; Gillen, J.; Daly, P.; Wolf, G. Comparison of single-shot localiation methods (STEAM and PRESS) for in vivo proton NMR spectroscopy. NMR in Biomedicine 2:201–208; 1989.
28. Nitsch, R.; Pittas, A.; Blusztajn, J. K.; Slack, B. E. Alterations of phospholipid metabolites in postmortem brain from patients with Alzheimer's disease. Ann. NY Acad. Sci. 640:110–113; 1991.
29. Nitsch, R. M.; Blusztajn, J. K.; Pittas, A. G. et al. Evidence for a membrane defect in Alzhiemer disease brain. Proc. Natl. Acad. Sci. 89:1671–1675; 1992.
30. O'Rahilly, R.; Muller, F. Developmental stages in human embryos. Carnegie Institution of Washington, Publication 637, pp. 81–92; 1987.
31. Richards, T. Proton MR Spectroscopy in multiple sclerosis: Value in establishing diagnosis, monitoring progression, and evaluating therapy. Am. J. Radiol. 157:1073–1078; 1991.
32. Schambra, U. B.; Lauder, J. M.; Petrusz, P.; Sulik, K. K. Development of neurotransmitter systems in the mouse embryo following acute ethanol exposure: A histological and immunocytochemical study. Int. J. Dev. Neurosci. 8:507–522; 1990.
33. Siebert, J. R.; Astley, S. J.; Clarren, S. K. Holoprosencephaly in a fetal macaque (Macaca nemestrina) following weekly exposure to ethanol. Teratol. 44:29–36; 1991.
34. Sulik, K. K.; Johnston, M. C.; Webb, M. A. Fetal alcohol syndrome: Embryogenesis in a mouse model. Science 214:936–938; 1981.
35. Sulik, K. K.; Johnston, M. C. Sequence of developmental alterations following acute ethanol exposure in mice. Craniofacial features of the fetal alcohol syndrome. Am. J. Anat. 166:257–269; 1983.
36. Sulik, K. K.; Johnston, M. C. Embryonic origin of holoprosencephaly: Interrelationship of the developing brain and face. Scanning Electron Microsc. 1:309–322; 1982.
37. Tunggal, B.; Hofmann, K.; Stoffel, W. In vivo ^{13}C nuclear magnetic resonance investigations of choline metabolism in rabbit brain. Magn. Res. Med. 13:90–102; 1990.
38. Vinters, H.; Miller, B. L.; Pardridge, W. Brain amyloid and Alzheimer disease. Ann. Int. Med. 109:41–54; 1988.
39. Wurtman, R. J.; Bluszajn, J. K.; Maire, J. C. "Autocannibalism" of choline-containing membrane phospholipids in the pathogenesis of Alzheimer's disease-a hypothesis. Neurochem. Int. 7:369–72; 1985.